

Game-theoretic Decentralized Coordination for Airspace Sector Overload Mitigation

Jaehan Im^a, Daniel Delahaye^b, David Fridovich-Keil^a, Ufuk Topcu^a

^a*The University of Texas at Austin, 110 Inner Campus Drive, Austin, 78712, Texas, United States*

^b*École Nationale de l'Aviation Civile, 7 Avenue Édouard Belin, CS 54005, Toulouse Cedex 4, 31055, France*

Abstract

Decentralized air traffic management systems offer a scalable alternative to centralized control, but often assume high levels of cooperation. In practice, such assumptions frequently break down since airspace sectors operate independently and prioritize local objectives. We address the problem of sector overload in decentralized air traffic management by proposing a mechanism that models self-interested behaviors based on best response dynamics. Each sector adjusts the departure times of flights under its control to reduce its own congestion, without any shared decision making. A tunable cooperativeness factor models the degree to which each sector is willing to reduce overload in other sectors. We prove that the proposed mechanism satisfies a potential game structure, ensuring that best response dynamics converge to a pure Nash equilibrium, under a mild restriction. In addition, we identify a sufficient condition under which an overload-free solution corresponds to a global minimizer of the potential function. Numerical experiments using 24 hours of European flight data demonstrate that the proposed algorithm substantially reduces overload even with only minimal cooperation between sectors, while maintaining scalability and matching the solution quality of centralized solvers.

Keywords: Air Traffic Management, Noncooperative Coordination, Game Theory, Potential Game, Decentralized System, Sector Overload

1. Introduction

Decentralized approaches to air traffic management (ATM) are gaining attention as scalable alternatives to centralized control [1, 2, 3, 4, 5], due to the increasing complexity of air traffic. These approaches often rely on *collaborative decision-making*, which assumes that stakeholders are willing to share information and cooperate toward a joint solution [3, 6, 7, 8, 9]. However, such assumptions frequently fail in practice, as neighboring airspace sectors often operate independently with limited data exchange and coordination [10, 11, 12, 13]. Consequently, modeling the ATM system as a cooperative multi-agent process can misrepresent the actual interactions between sector managers, who may prioritize local objectives over system-wide outcomes.

A key operational challenge in such decentralized settings is managing sector overload, which occurs when the number of aircraft in a sector exceeds a given capacity [14, 15, 16]. This leads to safety risks and increased controller workload [15, 16], and typically requires flight plan adjustments [9, 17, 18]. These interdependencies create a multi-agent decision-making problem, where each sectors action influences the congestion experienced by others.

We propose a decentralized mechanism that mitigates sector overloads by modeling sector interactions through a game-theoretic framework, capturing the full range from self-interested to cooperative behaviors. Each sector updates its decisions using best-response dynamics, myopically adjusting the departure times of flights under its control to reduce its own congestion without regard to others objectives. To capture varying levels of cooperative behavior, we introduce an adjustable *cooperativeness factor* κ , which interpolates between fully self-interested ($\kappa = 0$) and fully cooperative ($\kappa = 1$) behavior. This formulation enables us to analyze how limited cooperation can affect overall system performance without requiring full coordination.

We provide theoretical guarantees on the convergence of best-response dynamics in this setting. Specifically, we show that for $\kappa = 0$ or 1 , the game is a potential game, and best-response dynamics converges to a pure Nash equilibrium unconditionally. For intermediate values ($0 < \kappa < 1$), we prove that best-response dynamics converge in finitely many rounds under a mild restriction on update rules: sectors must avoid actions that introduce new overloads in other sectors. Additionally, we identify a sufficient condition under which any feasible solution (one with no sector overload) corresponds to a global minimizer of the potential function, providing insight into when the algorithm yields overload-free outcomes.

We validate the approach through numerical experiments using 24 hours of real flight data from the European airspace. Results show that even with a minimal level of *self-prioritizing* cooperation—where each sector agrees to a cooperative decision only if it does not compromise its own overload—the proposed decentralized algorithm remains scalable and produces solutions with quality comparable to those of the centralized solver. In addition, it achieves substantial reductions in sector overload compared to first-come-first-served heuristics.

In summary, the proposed algorithm models sector overload mitigation as a game with a tunable cooperativeness factor. We prove that it converges under best-response dynamics to pure Nash equilibria, and we demonstrate using real-world data that significant overload reduction can be achieved even with only very limited cooperation. The remainder of the paper reviews related work, presents the model and theoretical results, describes the experimental setup, and reports the numerical findings before concluding.

2. Related Work

2.1. Centralized approaches in ATM

A core challenge in ATM is *demandcapacity balancing*, the process of aligning air traffic demand with sector capacities to prevent overload [4, 9, 18]. Centralized approaches rely on a central authority with access to system-wide information to prevent congestion and coordinate schedules across sectors. Prominent methods include air traffic flow management [19] and performance-based ATM [3], which often use optimization models to minimize delay and promote fairness [3, 4, 18, 19, 20]. While effective in controlled settings, centralized schemes face scalability challenges as traffic grows and operations become more complex and heterogeneous, and such centralized ATFM is not feasible in some regions Asian airspace being a representative example [3, 4, 18, 19, 20].

2.2. Decentralized ATM and collaborative frameworks

To address these limitations, decentralized concepts have been explored through multi-agent frameworks and distributed trajectory management. *Collaborative decision-making* is a representative approach in this area, promoting negotiation and shared situational awareness among

stakeholders to improve outcomes [2, 5, 6, 7]—indeed collaborative decision-making has been successfully deployed in the United States [21] and the *Airport-CDM* systems at major European airports [22], supported by the network manager in Brussels. However, many decentralized approaches assume a high degree of transparency and willingness to cooperate assumptions that often fail in practice due to competitive dynamics and the noncooperative nature of ATM stakeholders, particularly in international or boundary airspace sectors [11].

2.3. Game-theoretic perspectives and limitations

Game theory has been increasingly adopted to model the strategic interdependence among ATM stakeholders such as airlines, controllers, and sectors [3, 23, 24, 25, 26, 27, 28]. These models capture both cooperative and competitive behaviors, and have been applied to areas ranging from congestion pricing [3] and trajectory negotiation [29, 30], to nation-scale ATM network optimization [31].

Despite this progress, most studies still presume a high level of cooperativeness or the presence of a central planner [3, 29, 30]. Explicit treatment of limited cooperation or self-interested coordination remains scarce [5, 24, 25, 28], even though case studies at flight information region (FIR) boundaries highlight persistent coordination gaps and operational inefficiencies [10, 12, 13]. Recent work suggests that while decentralized coordination shows promise [23], scalable implementations and strong theoretical guarantees for real-world ATM are still lacking [5, 11, 15, 24].

3. Airspace Sector Overload Problem

We formulate the sector overload resolution problem in terms of the agents, their decision variables, and the capacity constraints that should be respected. Figure 1 illustrates a simple example: a sector exceeding its capacity and the flight schedule adjustments removing overloads.

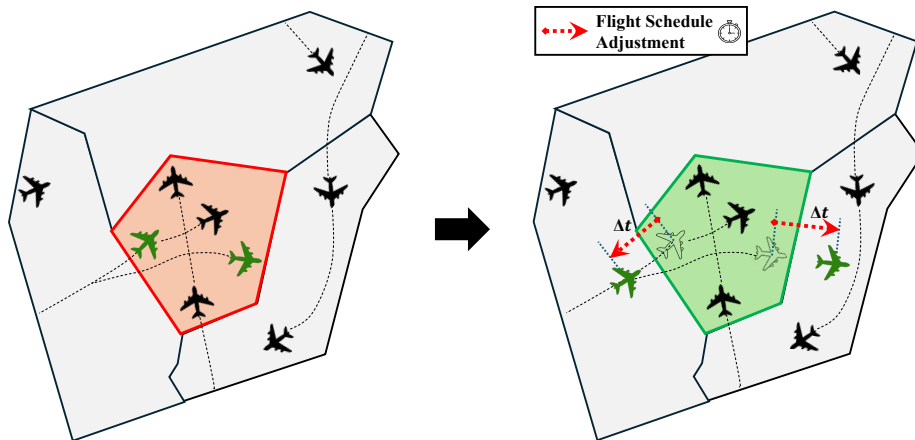


Figure 1: Illustration of sector overload mitigation. (Left) A sector with a capacity limit of three aircraft is overloaded with five active flights (red region). (Right) Two flights (green) adjust their flight schedule (red dashed arrows), removing the overload and restoring the sector to a feasible state (green region).

3.1. Airspace system and agents

The airspace is partitioned into m sectors, each managed by a local controller. We denote the set of sectors by $\mathbf{M} = \{1, \dots, m\}$. Sector $i \in \mathbf{M}$ manages n_i flights, and the total number of flights is $n = \sum_{i \in \mathbf{M}} n_i$. Each sector can adjust the departure times of its flights within a finite action set $\mathcal{A} \subset \mathbb{R}$, consisting of p discrete scheduling options. For example, $\mathcal{A} = \{0, 5, 10, 15, 20, 25, 30\}$ (minutes) represents departure-time adjustments in 5-minute increments over a 0 to 30 minute range. The decision variable of sector i is then $x_i \in \mathcal{A}_i := \mathcal{A}^{n_i}$, and the joint action profile across all sectors is $\mathbf{x} = (x_1, \dots, x_m) \in \bigcup_{i \in \mathbf{M}} \mathcal{A}_i = \mathcal{A}^{\sum_i n_i} = \mathcal{A}^n$.

3.2. Occupancy metric and overload definition

We measure sector overload using the *occupancy metric* defined as the number of aircraft present in a sector at a given time [32, 33]. Let $D_i \in \mathbb{Z}_{>0}$ denote the capacity of sector i , and let $C_{ji} : \mathcal{A}^n \rightarrow \mathbb{R}_{\geq 0}$ represent the contribution of flights scheduled by sector j to the load of sector i . The total load in sector i is $\sum_{j \in \mathbf{M}} C_{ji}(\mathbf{x})$. The *overload* in sector i , $L_i : \mathcal{A}^n \rightarrow \mathbb{R}_{\geq 0}$, is then defined as:

$$L_i(\mathbf{x}) = \max \left(0, \sum_{j \in \mathbf{M}} C_{ji}(\mathbf{x}) - D_i \right), \quad \mathbf{x} \in \mathcal{A}^n. \quad (1)$$

A solution $\mathbf{x}^* \in \mathcal{A}^n$ is *feasible* if all sectors respect their capacity constraints, i.e.,

$$\sum_{i \in \mathbf{M}} L_i(\mathbf{x}^*) = 0. \quad (2)$$

In other words, (1) measures a specific sector's overload, and (2) defines feasibility as complete elimination of overload across the system.

3.3. Action updates and local effects

Consider a unilateral update by agent i , denoted $\mathbf{x}'_i = (x_1, \dots, x'_i, \dots, x_m)$ for $x'_i \in \mathcal{A}_i$. Under the occupancy metric, the update affects only the contribution incurred by sector i . Accordingly,

$$C_{ji}(\mathbf{x}) = C_{ji}(\mathbf{x}'_i), \quad \mathbf{x} \in \mathcal{A}^n, \quad \forall j \neq i, \quad (3)$$

$$C_{jk}(\mathbf{x}) = C_{jk}(\mathbf{x}'_i), \quad \mathbf{x} \in \mathcal{A}^n, \quad \forall j, k \neq i. \quad (4)$$

Thus, only C_{ii} and C_{ij} (for $j \neq i$) may change when agent i updates its decision. This property will be central to the game-theoretic analysis in the next section.

3.4. Operational requirements and assumptions

The mechanism we seek must align with operational realities of decentralized ATM:

- **Local decision-making:** Each sector acts independently using only local information, without assuming centralized control or full information exchange.
- **Deterministic decision:** The resulting decisions must form a pure Nash equilibrium, ensuring predictable and stable schedules as required in ATM operations. Mixed-strategy equilibria would yield randomized schedules, which are not acceptable in safety-critical systems.
- **Finite-time overload resolution:** The mechanism must guarantee convergence within a finite number of steps to allow timely mitigation of overload situations.

3.5. Problem definition

Based on this structure, we define the *sector overload problem* as determining a joint action profile \mathbf{x}^* that eliminates all overload, i.e., identify departure-time adjustments for all flights that satisfies the feasibility condition in (2). Building on this formulation, the next section introduces our game model and establishes its theoretical properties.

4. Game-Theoretic Model of Sector Interaction

We model the sector overload problem as a game in which each sector is treated as an individual agent. We adopt *best-response dynamics* as the update rule: each sector independently adjusts its own schedule using only local information, without relying on centralized coordination. Best-response dynamics naturally mirrors how sector controllers make reactive decisions in practice.

Definition 1 (Best-response dynamics [34, 35]). *For a game involving m agents with cost functions $J_i : \mathcal{A}^n \rightarrow \mathbb{R}$ for $i \in \{1, \dots, m\}$ and action sets $\{\mathcal{A}_i\}_{i=1}^m$, the best-response mapping of agent i , $BR_i : \mathcal{A}^n \rightarrow \mathcal{A}_i$, is defined as:*

$$BR_i(\mathbf{x}) := \arg \min_{a \in \mathcal{A}_i} J_i(a, \mathbf{x}_{-i}), \quad \mathbf{x} \in \mathcal{A}^n, \quad (5)$$

where $\mathbf{x}_{-i} = (x_1, \dots, x_{i-1}, x_{i+1}, \dots, x_m)$. The best-response dynamics generates a sequence $\{\mathbf{x}^{(t)}\}_{t \geq 0}$ such that, at round t , one agent i unilaterally updates its decision according to

$$x_i^{(t+1)} \in BR_i(\mathbf{x}^{(t)}). \quad (6)$$

The best-response dynamics is known to converge to a pure Nash equilibrium in *potential games* [36, 34, 35], provided that the action space is finite, as in our case.

Definition 2 (Potential game [34]). *A game involving m agents with cost functions $\{J_i : \mathcal{A}^n \rightarrow \mathbb{R}\}_{i=1}^m$ is a potential game if there exists a potential function $\Phi : \mathcal{A}^n \rightarrow \mathbb{R}$ such that, for any agent i and any $\mathbf{x}'_i \in \mathcal{A}_i$, where $\mathbf{x}'_i = (x_1, \dots, x'_i, \dots, x_m)$,*

$$J_i(\mathbf{x}'_i) - J_i(\mathbf{x}) = \Phi(\mathbf{x}'_i) - \Phi(\mathbf{x}), \quad \mathbf{x} \in \mathcal{A}^n. \quad (7)$$

That is, the change in an agent's cost from a unilateral deviation exactly matches the change in the potential function. The potential function provides a global measure aligned with individual incentives, so unilateral improvements correspond to decreasing this function. Hence, its local minima coincide with pure Nash equilibria.

Since pure Nash equilibria correspond to reliable, deterministic decisions, showing that our model satisfies a potential function will ensure that it meets the operational requirements of ATM systems.

The remainder of this section develops as follows: (i) We first introduce a cost function with a tunable cooperativeness factor κ . (ii) We then establish conditions under which the game admits a potential structure and prove finite termination under a mild restriction for $0 < \kappa < 1$. (iii) Finally, we prove that best-response dynamics converges to a pure Nash equilibrium and identify when overload-free solutions are global minimizers of the potential function.

4.1. Cost function and cooperativeness factor κ

We define the cost function of sector $i \in \mathbf{M}$, $J_i : \mathcal{A}^n \rightarrow \mathbb{R}$, as

$$J_i(\mathbf{x}) = L_i(\mathbf{x}) + \kappa \sum_{j \in \mathbf{M} \setminus \{i\}} L_j(\mathbf{x}), \quad \mathbf{x} \in \mathcal{A}^n, \quad (8)$$

where $L_i(\mathbf{x})$ is the overload in sector i defined in (1), and $0 \leq \kappa \leq 1$ is the cooperativeness factor. The first term reflects each agents self-interest, while the second introduces a penalty for system-wide overload. This formulation interpolates between fully self-interested behavior ($\kappa = 0$) and fully cooperative behavior ($\kappa = 1$). In particular, we identify a special regime called *self-prioritizing cooperativeness*.

Definition 3 (Self-prioritizing cooperative behavior). *A sector i exhibits self-prioritizing cooperative behavior if it adopts a cooperative action only when that action does not increase its own overload; that is,*

$$L_i(\mathbf{x}'_i(a)) \leq L_i(\mathbf{x}), \quad \mathbf{x} \in \mathcal{A}^n, \quad \forall a \in \mathcal{A}_i, \quad (9)$$

where $\mathbf{x}'_i(a) = (x_1, \dots, x_{i-1}, a, x_{i+1}, \dots, x_m)$.

The following theorem provides a sufficient condition on κ under which a sector exhibits this behavior.

Theorem 1 (Sufficient bound on κ for self-prioritization). *If*

$$\kappa < \frac{1}{n(m-1)}, \quad (10)$$

where m is the number of sectors and n is the total number of flights, then no sector will adopt a cooperative action that increases its own overload.

Proof. The proof is provided in Appendix A. \square

This condition ensures that the cooperative term in (8) never outweighs the self-interest term, and therefore agents remain self-prioritizing. The self-prioritizing regime represents the minimal form of cooperation beyond purely self-interested behavior: sectors are willing to take cooperative actions only when such actions do not worsen their own overload.

4.2. Potential game properties

We now examine whether the game defined by (8) admits a potential function. We begin by considering the case where the set of overloaded sectors remains fixed.

Theorem 2 (Potential game under fixed overload set). *Let $\mathbf{M}_o : \mathcal{A}^n \rightarrow 2^{\mathbf{M}}$ denote the set of overloaded sectors, defined by:*

$$\mathbf{M}_o(\mathbf{x}) := \{i \in \mathbf{M} \mid L_i(\mathbf{x}) > 0\}, \quad \mathbf{x} \in \mathcal{A}^n. \quad (11)$$

If this set of overloaded sectors remains unchanged under unilateral deviations, then the game with cost function (8) admits the potential function $\Phi : \mathcal{A}^n \rightarrow \mathbb{R}$,

$$\Phi(\mathbf{x}) = \kappa \sum_{i \in \mathbf{M}} L_i(\mathbf{x}) + (1 - \kappa) \sum_{i \in \mathbf{M}_o(\mathbf{x})} C_{ii}(\mathbf{x}), \quad \mathbf{x} \in \mathcal{A}^n. \quad (12)$$

Proof. The proof is provided in Appendix A. \square

This means that, as long as unilateral deviations do not alter which sectors are overloaded, each agent's cost improvement aligns with a decrease in the global potential function.

Lemma 1 (Potential game for $\kappa = 0$ or $\kappa = 1$). *When $\kappa = 0$ or $\kappa = 1$, the game defined by (8) admits a potential function unconditionally.*

Proof. The proof is provided in Appendix A. \square

Unlike Theorem 2, this result holds regardless of how the overload set changes. In particular, for $\kappa = 1$ the potential function reduces to measuring only the system-wide overload, *i.e.* $\Phi(\mathbf{x}) = \sum_{i \in \mathbf{M}} L_i(\mathbf{x}) \geq 0$, so every feasible solution \mathbf{x}^* (*i.e.*, satisfying (2) and eliminating all system-wide overload) is a global minimizer of Φ .

4.3. Termination guarantee and restricted mechanism

When $0 < \kappa < 1$, the game in (8) is not generally a potential game. However, even in this regime, we can guarantee finite termination of the best-response dynamics by imposing a mild restriction on agents' actions.

For a joint action profile \mathbf{x} and a unilateral deviation \mathbf{x}'_i , let $\mathbf{M}_f : \mathcal{A}^n \times \mathcal{A}^n \rightarrow 2^{\mathbf{M}}$ denote the set of sectors that become overloaded after the deviation:

$$\mathbf{M}_f(\mathbf{x}, \mathbf{x}'_i) := \{ j \in \mathbf{M} \mid L_j(\mathbf{x}) = 0, L_j(\mathbf{x}'_i) > 0 \}, \quad \mathbf{x} \in \mathcal{A}^n, \quad (13)$$

where $\mathbf{x}'_i := (x_1, \dots, x'_i, \dots, x_m)$ for some $x'_i \in \mathcal{A}_i$. We impose the following restriction.

Definition 4 (No-new-overload restriction). *Agents are restricted to actions \mathbf{x}'_i such that $\mathbf{M}_f(\mathbf{x}, \mathbf{x}'_i) = \emptyset$, *i.e.*, no new overload is created.*

Under this restriction, a unilateral deviation can only maintain or reduce the set of overloaded sectors but can never expand it. This allows us to establish the following property.

Lemma 2 (Monotonic decrease of the overloaded set). *If a unilateral deviation changes the overloaded set, that is, $\mathbf{M}_o(\mathbf{x}'_i) \neq \mathbf{M}_o(\mathbf{x})$, then its cardinality must strictly decrease:*

$$\mathbf{M}_o(\mathbf{x}'_i) \subsetneq \mathbf{M}_o(\mathbf{x}), \quad \mathbf{x} \in \mathcal{A}^n. \quad (14)$$

Proof. The proof is provided in Appendix A. \square

Lemma 2 implies that $\mathbf{M}_o(\mathbf{x})$ either remains unchanged or strictly decreases after each round. Since \mathbf{M} is finite, this monotone property directly implies finite termination.

Theorem 3 (Finite termination for $0 < \kappa < 1$). *Consider the game defined by the cost function (8). Under the no-new-overload restriction (Definition 4), the best-response dynamics terminates in finite time and converges to a pure Nash equilibrium.*

Proof. The proof is provided in Appendix A. \square

The termination follows from two observations. Let $\mathbf{x}^{(t)}$ denote the joint action profile at round t . While $\mathbf{M}_o(\mathbf{x}^{(t)})$ remains fixed, the problem is a potential game and the best-response dynamics converges by Theorem 2. If $\mathbf{M}_o(\mathbf{x}^{(t)})$ changes, Lemma 2 ensures that $\mathbf{M}_o(\mathbf{x}^{(t+1)})$ is a strict subset of $\mathbf{M}_o(\mathbf{x}^{(t)})$. Since \mathbf{M} is finite, the overloaded set can change at most $|\mathbf{M}|$ times, and the number of best-response iterations at any fixed $\mathbf{M}_o(\mathbf{x}^{(t)})$ is bounded. Therefore, the process must terminate in finite time.

4.4. Convergence of best-response dynamics

The convergence of the best-response dynamics follows directly from the potential structure and the monotonic evolution of the overloaded set $\mathbf{M}_o(\mathbf{x})$. Lemma 1 guarantees that the game is a potential game when $\kappa = 0$ or $\kappa = 1$, while Theorem 3 establishes finite termination for $0 < \kappa < 1$ under the no-new-overload restriction. We summarize these results in the following theorem.

Theorem 4 (Convergence under best-response dynamics). *Consider the best-response dynamics defined in Definition 1. Based on Theorem 2 and Theorem 3, the following statements hold:*

1. *When $\kappa = 0$ or $\kappa = 1$, the game admits a potential function, and best-response dynamics converges unconditionally to a pure Nash equilibrium in finite time.*
2. *When $0 < \kappa < 1$, if agents are restricted from actions that introduce new overloads, the best-response dynamics terminates in finite time and converges to a pure Nash equilibrium.*

In both cases, best-response dynamics is guaranteed to converge in a finite number of steps.

Proof. The proof is provided in Appendix A. \square

Theorem 4 establishes conditions that best-response dynamics converges to a pure Nash equilibrium in finite time across all regimes of κ with no-new-overload action restriction. This provides the key operational guarantee for decentralized overload mitigation, ensuring that interactions based on best responses always terminate in finite time and the outcome is deterministic.

4.5. Sufficient condition for feasibility

Beyond convergence, we examine how feasible overload-free solutions relate to the potential function. When $\kappa = 1$, cost function (8) and potential function (12) become identical, which leads to the following result.

Theorem 5 (Feasible solutions as global minimizers). *When $\kappa = 1$, any feasible solution \mathbf{x}^* satisfying $L_i(\mathbf{x}^*) = 0$ for all i is a global minimizer of (12), the potential function.*

Proof. The proof is provided in Appendix A. \square

Theorem 5 shows that under full cooperation, whenever a feasible solution exists, it coincides with a global minimizer of the potential function.

4.6. Connection to operational requirements

To summarize, our theoretical results directly address the operational requirements identified in Section 3. These properties underscore the suitability of our approach for real-world ATM deployment.

5. Decentralized Overload Mitigation Mechanism

Building on the game-theoretic model in Section 3, we propose a decentralized algorithm based on best-response dynamics to address the sector overload problem. Each sector updates its own decision variable only using local information about flights it manages and the current system-wide congestion, without requiring a centralized coordinator.

Algorithm 1: Decentralized overload mitigation

Input: Sectors \mathbf{M} , action sets $\{\mathcal{A}_i\}_{i \in \mathbf{M}}$, capacities $\{D_i\}_{i \in \mathbf{M}}$, cooperativeness factor $\kappa \in [0, 1]$, initial schedule $\mathbf{x}^{(0)}$

- 1 Compute $L(\mathbf{x}^{(t)})$ and $J_i(\mathbf{x}^{(t)})$ for all i ;
- 2 $t \leftarrow 0$;
- 3 $\text{Improved} \leftarrow \text{true}$;
- 4 **while** Improved **do**
- 5 $\text{Improved} \leftarrow \text{false}$;
- 6 **for** $i \in \mathbf{M}$ **do**
- 7 Use GA to solve (15);
- 8 Update $L(\mathbf{x}^{(t+1)})$, $J_i(\mathbf{x}^{(t+1)})$;
- 9 **if** updated **then**
- 10 $\text{Improved} \leftarrow \text{true}$;
- 11 $t \leftarrow t + 1$;
- 12 **if** $\sum_i L_i(\mathbf{x}^{(t)}) = 0$ **then**
- 13 **return** $\mathbf{x}^{(t)}$
- 14 **if not** Improved **then**
- 15 **return** $\mathbf{x}^{(t)}$
- 16 **return** $\mathbf{x}^{(t)}$

5.1. Algorithm overview

At round t , sectors update sequentially. When sector i is active, it searches for a unilateral update a that minimizes its cost J_i in (8), while keeping the other sectors actions fixed. The candidate joint action is denoted by $\mathbf{x}_i^{(t+1)}(a) = (x_1^{(t)}, \dots, x_{i-1}^{(t)}, a, x_{i+1}^{(t)}, \dots, x_m^{(t)})$. The best response a is approximated using a genetic algorithm (GA) optimizing over \mathcal{A}_i , subject to the no-new-overload constraint Definition 4. This process repeats until no agent can improve.

5.2. Best response action update

Given the other sectors actions at round t , sector i computes its best response by solving

$$\begin{aligned} x_i^{(t+1)} \in \arg \min_{a \in \mathcal{A}_i} \quad & L_i(\mathbf{x}_i^{(t+1)}(a)) + \kappa \sum_{j \in \mathbf{M} \setminus \{i\}} L_j(\mathbf{x}_i^{(t+1)}(a)) \\ \text{s.t.} \quad & L_j(\mathbf{x}) = 0 \implies L_j(\mathbf{x}_i^{(t+1)}(a)) = 0, \quad \forall j \in \mathbf{M}. \end{aligned} \quad (15)$$

That is, sector i minimizes its cost while respecting the restriction that no new overload may be introduced. This update rule corresponds to the best-response dynamics analyzed in Theorem 4.

The action space $\mathcal{A}_i = \mathcal{A}^{n_i}$ is discrete and combinatorial, making exhaustive enumeration impractical. We therefore approximate the solution of the optimization problem above using a genetic algorithm which directly embeds the constraint.

5.3. Termination condition

The algorithm terminates when either of two conditions is met: (i) a full round over all sectors yields no update, meaning no agent can further reduce its cost and we have reached a pure Nash equilibrium under Theorem 4; or (ii) a feasible overload-free solution is found mid-round, enabling early termination.

6. Numerical Experiments

We conduct numerical experiments to evaluate the performance of the proposed algorithm. The experiments are designed to answer three main questions: (i) how the cooperativeness factor κ affects algorithm performance, (ii) how the algorithm compares against representative baseline methods, and (iii) whether the method scales to scenarios with large numbers of flights. We first describe the experimental setup and baselines before presenting the results.

6.1. Experiment setup and data description

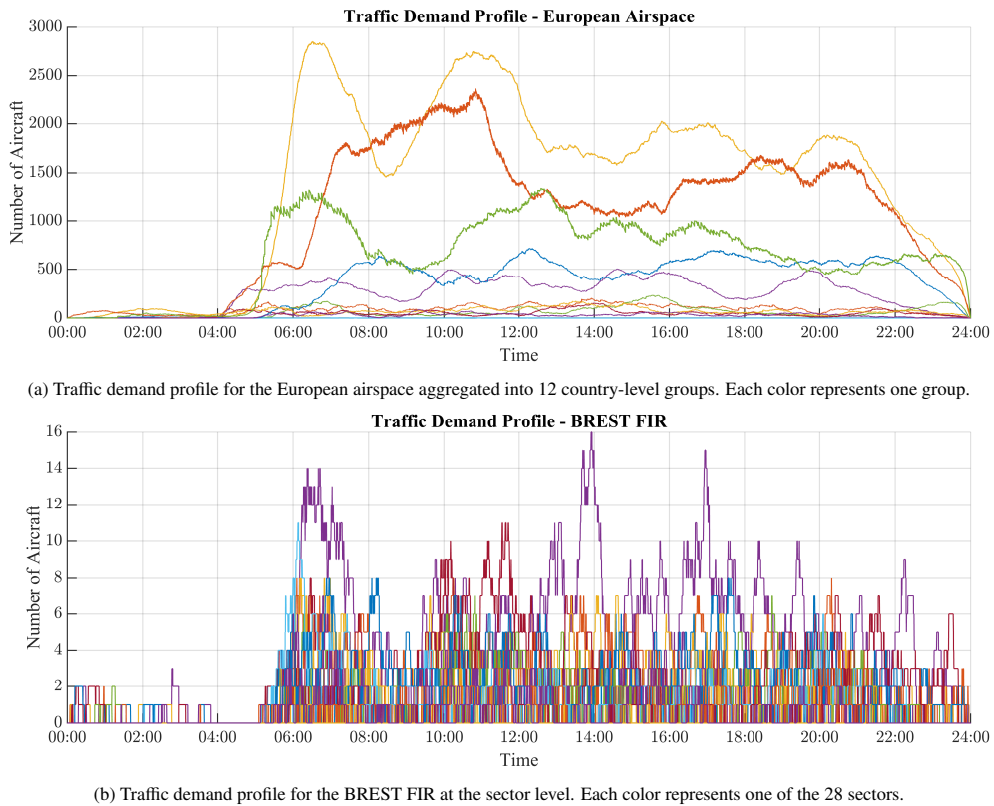


Figure 2: Traffic demand profiles on July 27, 2023. The plots illustrate temporal variations in traffic demand at two different levels of spatial aggregation: (a) European airspace grouped by 12 countries, and (b) BREST FIR divided into 28 individual sectors.

We evaluate the performance of the proposed algorithm using 24 hours of flight plan data from July 27, 2023 over the European airspace, which includes 42,783 flights and 1,128 regional sectors. Figure 2 illustrates the traffic demand profiles at two levels of aggregation: the entire European airspace grouped by 12 countries (Figure 2a) and the BREST flight information region (FIR) in France divided into 28 sectors (Figure 2b). Our main experiments focus on the BREST FIR, which contains 1,247 flights across 28 sectors. Each sector is assigned a uniform capacity limit $D_i = 10$ for all $i \in \{1, \dots, 28\}$.

Each flights action set is defined as discrete departure delays in 5-minute increments, ranging from 0 to 30 minutes: $\mathcal{A} = \{0, 5, 10, 15, 20, 25, 30\}$. Sector i action is $x_i \in \mathcal{A}_i := \mathcal{A}^{n_i}$ where we recall that n_i is the number of flights that sector i controls, and the joint action \mathbf{x} specifies the departure schedule for all flights.

The decentralized algorithm is tested with cooperativeness factors $\kappa \in \{0, 10^{-6}, 0.5, 1\}$, covering regimes from fully self-interested to fully cooperative. In particular, $\kappa = 10^{-6}$ satisfies the sufficient condition in Theorem 1 (since $10^{-6} < \frac{1}{n(m-1)} \approx 2.96 \times 10^{-5}$), corresponding to the *self-prioritizing cooperation*.¹ We include $\kappa = 0.5$ as an intermediate value to illustrate trade-offs between this regime and the fully cooperative case. For each setting, we conduct 10 Monte Carlo trials to account for the stochasticity of the genetic algorithm solver and runtime.

The BREST FIR dataset alone does not provide a sufficient number of flights for large-scale experiments. Thus, we use the full European dataset, grouping sectors by country and treating each as a sector-like agent, as illustrated in Figure 2a for the scalability test. We perform 10 Monte Carlo trials for each traffic volume, ranging from 10 to 10,000 aircraft, by randomly sampling the designated number of flights. Each agent is assigned a uniform capacity limit $D_i = D$, with D calibrated to represent 85% of the maximum observed overload in each scenario.

Implementation details. All experiments were implemented in MATLAB with identical genetic algorithm [37] hyperparameters (population size = 50, crossover / mutation rates = 0.8 / 0.1, maximum generations = 100). Experiments were conducted on a computer with an Intel Core i7-12700 processor and 16 GB RAM. Parallel computation was enabled, utilizing 19 threads.

6.2. Baselines

We compare the proposed decentralized algorithm against two representative benchmarks:

- 1) **Centralized solver:** The centralized solver simulates an idealized system-wide coordinator with authority to modify all flight plans. It solves:

$$\begin{aligned} \min_{\mathbf{x}} \quad & \sum_{i \in \mathbf{M}} L_i(\mathbf{x}) \\ \text{s.t.} \quad & x_i \in \mathcal{A}_i, \quad \forall i \in \mathbf{M}. \end{aligned} \tag{16}$$

We use the same genetic algorithm-based solver as in (15) for fair comparison. This benchmark represents a lower bound on system overload, assuming full information sharing and centralized authority.

- 2) **First-Come-First-Served (FCFS):** The FCFS heuristic represents a reactive baseline analogous to current tactical resolution practices. When an overload is detected, the imminent flight scheduled to enter the congested sector is delayed using the same discrete action set \mathcal{A} as in our model, until feasibility is restored or no further delay options remain. This heuristic captures the myopic, locally reactive behavior commonly used in todays ATM systems, without consideration of system-wide optimization.

6.3. Results

We now present the results of our numerical experiments, building on the setup and baselines described above.

¹ m denotes the number of sectors and n denotes the total number of flights (see Section 3).

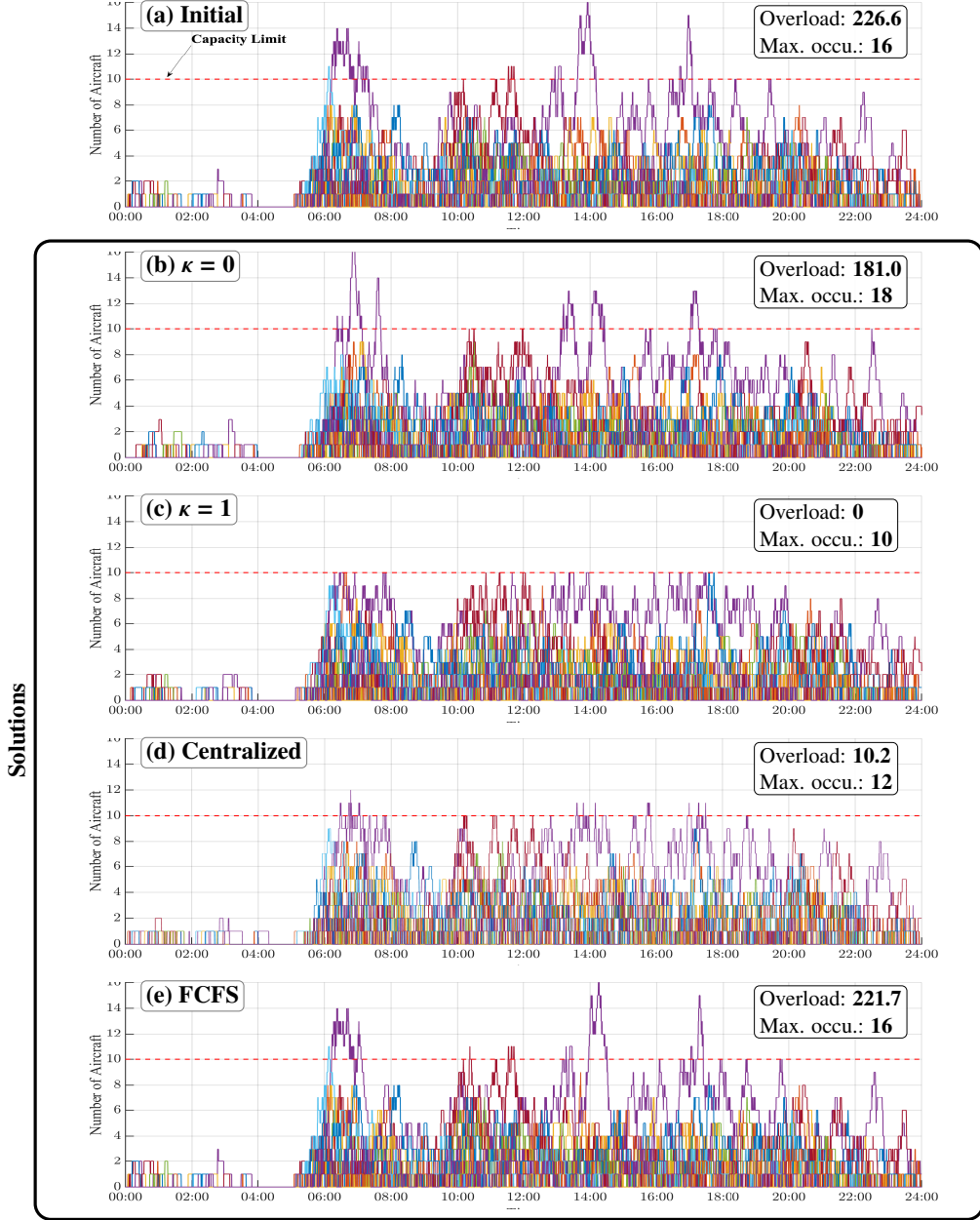


Figure 3: Traffic demand profiles in BREST FIR. Top (a): initial schedule. Bottom (be): outcomes under different cooperativeness factor (κ) settings and algorithms. Side boxes report solution quality measures: total overload [aircraft-min] and maximum instantaneous occupancy [number of aircraft].

6.3.1. Qualitative analysis

We first visually inspect how the proposed algorithm behaves under different κ values in a representative case from the BREST FIR dataset (Figure 3). When $\kappa = 1$, the algorithm eliminates all overload (i.e., occupancy never exceeds the threshold), producing solutions visually similar to the centralized benchmark (Figure 3c and Figure 3d). In contrast, $\kappa = 0$ leaves substantial overload unresolved, and the FCFS heuristic performs similarly (Figure 3b and Figure 3e). These observations suggest that high cooperation ($\kappa = 1$) enables the decentralized algorithm to remove overload effectively, even when the centralized solver does not always succeed in finding a strictly feasible solution. Having confirmed the algorithms behavior in representative cases, we next turn to Monte Carlo experiments for a more systematic evaluation, including intermediate values of $\kappa = 10^{-6}$ and 0.5.

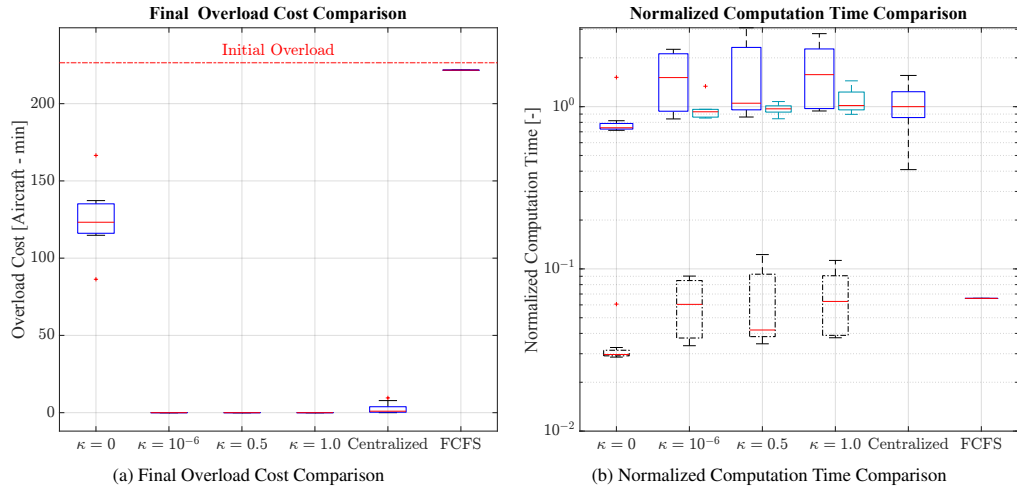


Figure 4: (a) Final overload cost comparison across κ values and baselines. A purely self-interested regime ($\kappa = 0$) leaves substantial overload unresolved, while other cooperation factors eliminate overload. (b) Normalized computation time comparison. Computation times are normalized by the median runtime of the centralized solver so that all results are shown on a common dimensionless scale. For the decentralized cases ($\kappa \in \{0, 10^{-6}, 0.5, 1.0\}$), the blue upper boxplots show the total runtime, while the lower dotted boxplots show the average runtime per sector. The green side boxplots indicate the time required for the decentralized algorithm to reach the overload level achieved by the centralized solver.

6.3.2. Effect of κ on the algorithm performance

The decentralized algorithm eliminates overload whenever $\kappa > 0$, whereas the fully self-interested case ($\kappa = 0$) reduces the initial overload by only about 47%. Even the self-prioritizing cooperation regime ($\kappa = 10^{-6}$) suffices to achieve overload-free solutions (Figure 4a).

With respect to computation time, $\kappa = 0$ converges the fastest among the decentralized cases due to premature termination, requiring roughly 47% of the runtime of the cooperative regimes. Nonzero κ values incur higher runtimes, as the algorithm requires additional rounds until the termination condition is satisfied.

6.3.3. Baseline comparison

Compared with centralized and heuristic baselines, the decentralized algorithm with $\kappa > 0$ consistently achieves overload-free solutions. The centralized solver reduces overload substan-

tially but often fails to reach a strictly feasible schedule, leaving a small residual overload, while the FCFS heuristic performs the worst, with only a 2.5% reduction on average (Figure 4a).

Computation times reveal a similar pattern: $\kappa = 0$ converges fastest, while $\kappa > 0$ cases require approximately 50-57% longer total runtime than the centralized solver (Figure 4b). Nevertheless, the decentralized algorithm reaches the overload level achieved by the centralized solver within a comparable time frame, requiring about 92101% of the centralized runtime. Because computation is distributed among agents, the per-agent effort remains on the order of $1/m$ of the centralized load, corresponding to only about 4-6% of the centralized solver’s total runtime.

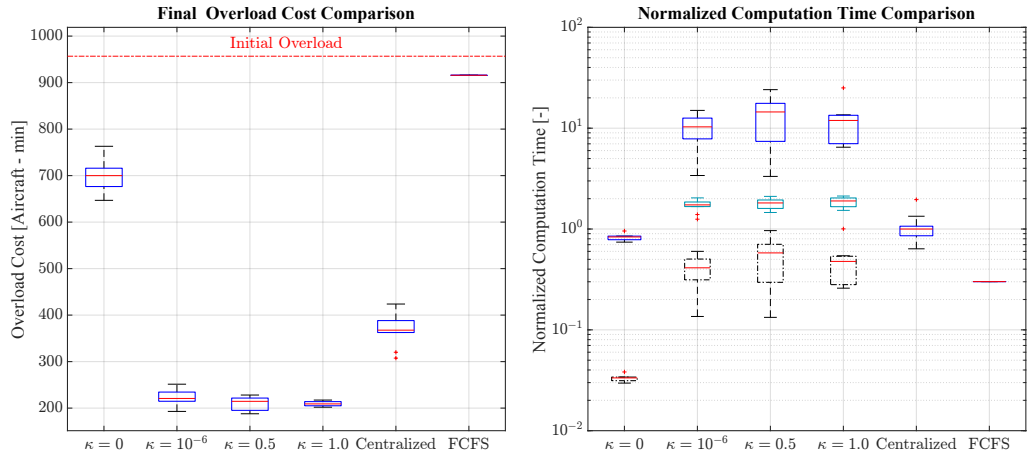


Figure 5: Stress test with reduced sector capacity ($D = 7$). (a) Final overload cost comparison. Unlike the $D = 10$ case where all $\kappa > 0$ values eliminated overload, here residual overload remains and performance differences between κ values become evident. (b) Normalized computation time comparison. Computation times are normalized by the median runtime of the centralized case. Nonzero κ values incur longer runtime, exceeding that of the centralized solver.

6.3.4. Stress test

As all $\kappa > 0$ cases in the $D = 10$ setting eliminate overload, we additionally evaluate a harder case where finding a feasible solution is difficult. Specifically, we repeat the BREST FIR experiments with a reduced capacity limit of $D = 7$, as illustrated in Figure 5.

In this setting, none of the methods consistently identify overload-free solutions. Across all trials, the performance ranking remains the same: the decentralized algorithm achieves the lowest residual overload, followed by the centralized solver, $\kappa = 0$, and FCFS. Among the $\kappa > 0$ cases, larger κ values tend to achieve smaller residual overloads. Even a minimal cooperation level ($\kappa = 10^{-6}$) substantially reduces total overload by 76.8%, while $\kappa = 1$ achieves the highest reduction of 78.3%. The centralized solver records a 60% reduction.

The runtime gap between the decentralized and centralized solvers becomes more pronounced in this setting. For $\kappa > 0$, the decentralized algorithm requires about 10-14 times longer total runtime than the centralized solver, as small yet persistent improvements in the solution lead to additional update rounds. In this setting, reaching the overload level achieved by the centralized solver takes longer, requiring about 1.7-1.9 times the centralized runtime. Nevertheless, the per-agent computational load remains below that of the centralized solver, since computation is distributed among agents.

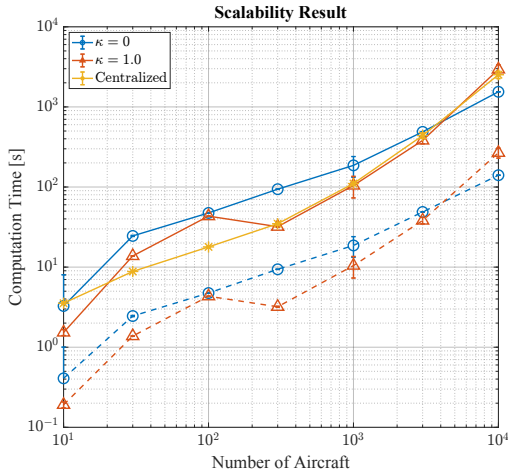


Figure 6: Scalability results comparing decentralized and centralized methods. Solid lines show total runtime, where both methods exhibit similar scaling behavior. Dashed lines show per-agent runtimes.

6.3.5. Scalability

We evaluate the scalability of the proposed algorithm with varying numbers of aircraft. To test scenarios involving larger traffic volumes, we utilize the full European dataset aggregated into 12 country-level agents with capacity limits set to 85% of the maximum observed overload, as described in Section 6.1. We sample 10 random instances for each traffic volume ranging from 10 to 10,000 flights.

As shown in Figure 6, the total runtimes of the decentralized algorithm (solid lines) scale similarly to those of the centralized solver across all problem sizes². The distribution of computation in decentralized algorithm leads to substantially lower per-agent runtimes (dashed lines), and the gap grows with the number of aircraft (note that Figure 6 is plotted on a log-log scale). This highlights the reduced computational burden per participant in the decentralized approach.

7. Discussion

7.1. Minimal cooperation as the key driver

Experiments show that the decentralized algorithm achieves effective overload mitigation with only a minimal degree of cooperation. The fully self-interested case ($\kappa = 0$) consistently fails, whereas the self-prioritizing regime ($\kappa = 10^{-6}$) already eliminates overload in the $D = 10$ setting as shown in Figure 4a. Thus, full altruism is unnecessary; a minimal willingness to act beyond ones own benefit suffices.

In terms of runtime, the decentralized algorithm scales similarly to the centralized solver in total runtime. Its distributed structure reduces per-agent computation in proportion to $1/m$. The self-interested case ($\kappa = 0$) terminates fastest, but only due to premature convergence to poor-quality solutions. Overall, even minimal cooperation can eliminate (cf. Figure 4) or substantially

²For $\kappa = 1.0$ and the centralized case, all instances resolve the overload, while $\kappa = 0$ fails to do so except in the 10-aircraft scenario.

reduce (cf. stress test in Figure 5) overload while matching the computation time scaling of the centralized approach.

7.2. Empirical performance versus theoretical guarantees

Theorem 5 guarantees that when $\kappa = 1$, the minimizer of the potential function corresponds to a feasible solution if such a solution exists. However, this does not ensure that best-response dynamics will actually reach such solution. In practice, our experiments show that feasible solutions were often obtained even for $\kappa \in (0, 1)$, outside the scope of the theoretical guarantee. This observation highlights the practical effectiveness of the algorithm and motivates future work closing the gap between theoretical guarantees and observed performance.

7.3. Implications for real-world deployment

Using real flight plan data, we demonstrated that the proposed decentralized algorithm effectively reduces overload. The finding that only minimal cooperation is required is particularly promising for decentralized ATM, where full cooperation is unrealistic. This suggests that effective coordination is achievable under realistic behavioral assumptions.

Remark 1 (On the centralized solver). *We deliberately used MATLABs built-in genetic algorithm [37] for both the decentralized and centralized formulations to ensure a fair comparison. The infeasibility observed in the centralized solver should not be interpreted as evidence that centralized methods are not suitable for real ATM problems; state-of-the-art integer programming solvers can reliably find feasible solutions for the BREST dataset within few seconds. Instead, the results highlight that, under identical solver assumptions, decentralization can aid metaheuristic search in finding high-quality solutions. Further details on the performance of state-of-the-art centralized solver are provided in Appendix B.*

8. Conclusion

We propose a game-theoretic mechanism for mitigating sector overload in decentralized air traffic management (ATM). The model introduces a tunable cooperativeness factor κ , which interpolates between fully self-interested behavior ($\kappa = 0$) and fully cooperative behavior ($\kappa = 1$). We show that the resulting game admits a potential structure in the extreme regimes ($\kappa = 0$ or 1) and that, for $0 < \kappa < 1$, best-response dynamics terminates in finite time under a no-new-overload restriction. Leveraging these properties, we prove that best-response dynamics converges to a pure Nash equilibrium.

Numerical experiments with real European flight data confirm the practical effectiveness of the approach. The algorithm eliminates or substantially reduce overload whenever $\kappa > 0$, even in cases with very small κ that induce agents to act altruistically only when it does not worsen their own overload. Stress tests with tighter capacities and scalability tests with up to 10,000 flights further show that the decentralized algorithm consistently produces solutions with less overload than centralized and heuristic baselines. At the same time, the proposed approach scales comparably in total runtime with the centralized approach while reducing per-agent computational burden.

These results highlight the central insight that effective decentralized coordination does not require full altruism. Minimal cooperation that does not compromise ones own interest is sufficient to achieve near-centralized performance in mitigating sector overload. Future work will

further strengthen theoretical guarantees for convergence to overload-free solutions. Future research directions include integrating the framework with rerouting strategies and extending it to account for various measures of sector complexity beyond the occupancy metric [32, 33], as well as incorporating uncertainties in demand and capacity forecasts.

CRediT authorship contribution statement

Jaehan Im: Conceptualization, Methodology, Software, Formal analysis, Writing original draft. **Daniel Delahaye:** Supervision, Resources, Validation, Writing review & editing. **David Fridovich-Keil:** Supervision, Funding acquisition, Methodology, Writing review & editing. **Ufuk Topcu:** Supervision, Funding acquisition, Methodology, Writing review & editing.

Declaration of competing interest

The authors declare that they have no known competing financial interests or personal relationships that could have appeared to influence the work reported in this paper.

Acknowledgments

This work was supported by the National Science Foundation CAREER award under grants 2336840 and 2211548, by the National Aeronautics and Space Administration ULI Award under grant 80NSSC21M0071, and by the Office of Naval Research under grant N00014-22-1-2703.

Data availability

The data that has been used is confidential.

Appendix A. Proofs for the theorems and lemmas

Proof of Theorem 1. Recall the cost function from (8):

$$J_i(\mathbf{x}) = L_i(\mathbf{x}) + \kappa \sum_{j \in \mathbf{M} \setminus \{i\}} L_j(\mathbf{x}). \quad (\text{A.1})$$

A deviation is *self-prioritizing* if sector i never adopts an action that increases its own overload, i.e.,

$$L_i(\mathbf{x}'_i(a)) \leq L_i(\mathbf{x}), \quad \forall a \in \mathcal{A}_i. \quad (\text{A.2})$$

Step 1. Cost difference under deviation. For a unilateral deviation $x_i \rightarrow x'_i$, define

$$\Delta L_i = L_i(\mathbf{x}'_i) - L_i(\mathbf{x}), \quad \Delta L_{-i} = \sum_{j \neq i} (L_j(\mathbf{x}'_i) - L_j(\mathbf{x})). \quad (\text{A.3})$$

Then

$$J_i(\mathbf{x}'_i) - J_i(\mathbf{x}) = \Delta L_i + \kappa \Delta L_{-i}. \quad (\text{A.4})$$

Step 2. Critical case when $\Delta L_i > 0$. If i 's own overload decreases ($\Delta L_i < 0$), the deviation is consistent with self-interest and poses no issue. The problematic case is $\Delta L_i > 0$: here sector i 's own overload increases. If simultaneously $\Delta L_{-i} < 0$ (i.e., other sectors overload decreases), the cooperative term $\kappa \Delta L_{-i}$ is negative and may outweigh ΔL_i , leading i to accept a deviation that harms itself.

Step 3. Worst-case bound on ΔL_{-i} . Each of the n flights controlled by i can affect up to $(m - 1)$ other sectors. Thus, in the worst case, $|\Delta L_{-i}| \leq n(m - 1)$. Since $\Delta L_i \geq 1$ whenever i 's overload increases, a sufficient condition for

$$\Delta J_i = \Delta L_i + \kappa \Delta L_{-i} > 0 \quad \text{whenever } \Delta L_i > 0 \quad (\text{A.5})$$

is

$$1 - \kappa n(m - 1) > 0. \quad (\text{A.6})$$

Step 4. Conclude. Hence, a sufficient bound for self-prioritization is

$$\kappa < \frac{1}{n(m - 1)}. \quad (\text{A.7})$$

Under this condition, the cooperative term never dominates the self-interest term, so no player adopts an action that raises its own overload. All players therefore behave in a self-prioritizing manner, completing the proof. \square

Proof of Theorem 2. Recall the cost function in (8):

$$J_i(\mathbf{x}) = L_i(\mathbf{x}) + \kappa \sum_{j \neq i} L_j(\mathbf{x}). \quad (\text{A.8})$$

Suppose the set of overloaded sectors $\mathbf{M}_o(\mathbf{x}) = \{i \mid L_i(\mathbf{x}) > 0\}$ remains unchanged under a unilateral deviation.

Step 1. Expand the cost difference. For player i changing its action from x_i to x'_i ,

$$J_i(\mathbf{x}'_i) - J_i(\mathbf{x}) = \sum_{j \in \mathbf{M}} (C_{ji}(\mathbf{x}'_i) - C_{ji}(\mathbf{x})) + \kappa \sum_{j \in \mathbf{M}_o \setminus \{i\}} \sum_{k \in \mathbf{M}} (C_{kj}(\mathbf{x}'_i) - C_{kj}(\mathbf{x})). \quad (\text{A.9})$$

Step 2. Use invariance properties. From Equations (3) and (4), all terms with $j \neq i$ or $k \neq i$ cancel, leaving

$$J_i(\mathbf{x}'_i) - J_i(\mathbf{x}) = (1 - \kappa)(C_{ii}(\mathbf{x}'_i) - C_{ii}(\mathbf{x})) + \kappa \sum_{j \in \mathbf{M}_o} (C_{ij}(\mathbf{x}'_i) - C_{ij}(\mathbf{x})). \quad (\text{A.10})$$

Step 3. Expand the potential function. Define

$$\Phi(\mathbf{x}) = \kappa \sum_{i \in \mathbf{M}} L_i(\mathbf{x}) + (1 - \kappa) \sum_{i \in \mathbf{M}_o} C_{ii}(\mathbf{x}). \quad (\text{A.11})$$

The potential difference under $\mathbf{x} \rightarrow \mathbf{x}'_i$ is

$$\Phi(\mathbf{x}'_i) - \Phi(\mathbf{x}) = (1 - \kappa)(C_{ii}(\mathbf{x}'_i) - C_{ii}(\mathbf{x})) + \kappa \sum_{j \in \mathbf{M}_o} (C_{ij}(\mathbf{x}'_i) - C_{ij}(\mathbf{x})). \quad (\text{A.12})$$

Step 4. Compare. Thus

$$J_i(\mathbf{x}'_i) - J_i(\mathbf{x}) = \Phi(\mathbf{x}'_i) - \Phi(\mathbf{x}). \quad (\text{A.13})$$

So Φ is a potential function whenever \mathbf{M}_o remains fixed. \square

Proof of Lemma 1. Case 1: $\kappa = 0$. Each players cost reduces to its own overload:

$$J_i(\mathbf{x}) = L_i(\mathbf{x}). \quad (\text{A.14})$$

A potential function is simply

$$\Phi(\mathbf{x}) = \sum_{i \in \mathbf{M}} L_i(\mathbf{x}), \quad (\text{A.15})$$

because any unilateral deviation changes exactly the deviators overload by the same amount as the global sum.

Case 2: $\kappa = 1$. Each players cost becomes

$$J_i(\mathbf{x}) = \sum_{j \in \mathbf{M}} L_j(\mathbf{x}), \quad \forall i, \quad (\text{A.16})$$

which is identical for all players and equals

$$\Phi(\mathbf{x}) = \sum_{j \in \mathbf{M}} L_j(\mathbf{x}). \quad (\text{A.17})$$

Therefore the game is a potential game with Φ as the potential function. Thus, for both $\kappa = 0$ and $\kappa = 1$, the potential structure holds unconditionally. \square

Proof of Lemma 2. Let $\mathbf{M}_o(\mathbf{x})$ denote the set of overloaded sectors before a unilateral deviation by agent i , and let $\mathbf{M}_o(\mathbf{x}'_i)$ denote the corresponding set after the deviation. Under the no-new-overload restriction (Definition 4), no sector that was previously feasible can become overloaded, that is, $\mathbf{M}_f(\mathbf{x}, \mathbf{x}'_i) = \emptyset$. Hence, $\mathbf{M}_o(\mathbf{x}'_i) \subseteq \mathbf{M}_o(\mathbf{x})$ and $|\mathbf{M}_o(\mathbf{x}'_i)| \leq |\mathbf{M}_o(\mathbf{x})|$. \square

Proof of Theorem 3. Let $\mathbf{x}^{(t)}$ denote the joint action profile and $\mathbf{M}_o^{(t)}$ the set of overloaded sectors at round t . Two situations may occur during the best response dynamics:

1. **\mathbf{M}_o remains fixed:** When $\mathbf{M}_o^{(t+1)} = \mathbf{M}_o^{(t)}$, the game behaves as a potential game by Theorem 2, and the best response dynamics converges to a pure Nash equilibrium in finite time.
2. **\mathbf{M}_o changes:** If $\mathbf{M}_o^{(t+1)} \neq \mathbf{M}_o^{(t)}$, then by Lemma 2 it must strictly decrease, $\mathbf{M}_o^{(t+1)} \subsetneq \mathbf{M}_o^{(t)}$. This change occurs before convergence under the previous fixed-overload configuration, which itself would be reached in finite time, and such reductions can occur only finitely many times because \mathbf{M} is finite. Once $\mathbf{M}_o^{(t)} = \emptyset$, all sector constraints are satisfied, corresponding to a stable equilibrium, and the algorithm terminates.

Whenever the overloaded set changes at round t , a new fixed configuration $\mathbf{M}_o^{(t+1)}$ is established, and the above two cases repeat. Since each step either converges under a fixed configuration or strictly reduces \mathbf{M}_o , the overall process must terminate in finite time. \square

Proof of Theorem 4. We leverage the results from Lemma 1 and Theorem 3.

1. **If $\kappa = 0$ or $\kappa = 1$:** By Lemma 1, the game is a potential game, so the best response dynamics monotonically decreases the potential function and converges unconditionally to a pure Nash equilibrium in finite time.
2. **If $0 < \kappa < 1$:** By Theorem 3, under the restriction $\mathbf{M}_f = \emptyset$, the best response dynamics terminates in finite time. At termination, no agent can unilaterally improve its cost, implying that the final joint action constitutes a pure Nash equilibrium.

Hence, in all regimes of κ , the best response dynamics converges to a pure Nash equilibrium within finite time. \square

Proof of Theorem 5. For $\kappa = 1$, the cost function simplifies to

$$J_i(\mathbf{x}) = \sum_{j \in \mathbf{M}} L_j(\mathbf{x}), \quad \forall i, \quad (\text{A.18})$$

and the potential function is the same:

$$\Phi(\mathbf{x}) = \sum_{j \in \mathbf{M}} L_j(\mathbf{x}). \quad (\text{A.19})$$

If \mathbf{x}^* is feasible, then $L_j(\mathbf{x}^*) = 0$ for all j , hence

$$\Phi(\mathbf{x}^*) = 0. \quad (\text{A.20})$$

Because overloads are nonnegative, 0 is the minimum possible value of Φ . Therefore any feasible solution is a global minimizer of the potential. \square

Appendix B. Performance of state-of-the-art centralized solver

The sector overload congestion mitigation algorithm [38] was tested on the BREST FIR dataset with $D = 10$. The solver, implemented in Java, achieved convergence with no remaining conflicts within 0.065 seconds on a MacBook Air equipped with an 8-core Apple M2 processor and 16 GB RAM.

References

- [1] I. R. de Oliveira, E. Carlos Pinto Neto, T. T. Matsumoto, H. Yu, Decentralized air traffic management for advanced air mobility, in: 2021 Integrated Communications Navigation and Surveillance Conference (ICNS), 2021, pp. 1–8. doi:10.1109/ICNS52807.2021.9441552.
- [2] A. Bicchi, A. Marigo, G. Pappas, M. Pardini, G. Parlangeli, C. Tomlin, S. Sastry, Decentralized air traffic management systems: Performance and fault tolerance, IFAC Proceedings Volumes 31 (1998) 259–264. doi:https://doi.org/10.1016/S1474-6670(17)40038-3, iFAC Workshop on Motion Control (MC’98), Grenoble, France, 21-23 September.
- [3] A. Evans, V. Vaze, C. Barnhart, Airline-driven performance-based air traffic management: Game theoretic models and multicriteria evaluation, Transportation Science 50 (2016) 180–203.

[4] J.-R. Künnen, A. K. Strauss, N. Ivanov, R. Jovanovi, F. Fichert, Leveraging demand-capacity balancing to reduce air traffic emissions and improve overall network performance, *Transportation Research Part A: Policy and Practice* 174 (2023) 103716. doi:<https://doi.org/10.1016/j.tra.2023.103716>.

[5] M. Nguyen-Duc, J.-P. Briot, A. Drogoul, An application of multi-agent coordination techniques in air traffic management, in: *IEEE/WIC International Conference on Intelligent Agent Technology*, 2003. IAT 2003., 2003, pp. 622–625. doi:[10.1109/IAT.2003.1241159](https://doi.org/10.1109/IAT.2003.1241159).

[6] M. O. Ball, C.-Y. Chen, R. Hoffman, T. Vossen, Collaborative decision making in air traffic management: Current and future research directions, in: L. Bianco, P. Dell'Olmo, A. R. Odoni (Eds.), *New Concepts and Methods in Air Traffic Management*, Springer Berlin Heidelberg, Berlin, Heidelberg, 2001, pp. 17–30.

[7] H. Oberheid, D. Soffker, Designing for cooperation - mechanisms and procedures for air-ground integrated arrival management, in: *2007 IEEE International Conference on Systems, Man and Cybernetics*, 2007, pp. 253–259. doi:[10.1109/ICSMC.2007.4414108](https://doi.org/10.1109/ICSMC.2007.4414108).

[8] M. Adams, S. Kolitz, A. Adani, Evolutionary concepts for decentralized air traffic flow management, in: *Guidance, Navigation, and Control Conference*, 1997, p. 3857.

[9] Y. Xu, R. Dalmau, M. Melgosa, A. Montlaur, X. Prats, A framework for collaborative air traffic flow management minimizing costs for airspace users: Enabling trajectory options and flexible pre-tactical delay management, *Transportation Research Part B: Methodological* 134 (2020) 229–255.

[10] D. Connolly, A. M. Hynd, The construction and enforcement of east asias air defence identification zones: Grey volumes in the sky?, *Environment and Planning C: Politics and Space* 41 (2023) 1029–1046.

[11] L. Adacher, M. Flamini, E. Romano, Sectors co-operation in air traffic management, *IFAC-PapersOnLine* 50 (2017) 4222–4227.

[12] A. R. Arafah, A. T. Tjitrawati, A. N. Bais, F. H. Nurkhalisha, Fir agreement indonesia-singapore: What are the legal implications?, *Heliyon* 10 (2024).

[13] T. HIRATA, H. KINOSHITA, Simulation analysis of the conflicts among the international departure flights from asian region over pacific oceanic airspace, *Journal of the Eastern Asia Society for Transportation Studies* 13 (2019) 2307–2319.

[14] J. Djokic, B. Lorenz, H. Fricke, Air traffic control complexity as workload driver, *Transportation Research Part C: Emerging Technologies* 18 (2010) 930–936. doi:<https://doi.org/10.1016/j.trc.2010.03.005>, special issue on *Transportation Simulation Advances in Air Transportation Research*.

[15] M. Janić, A model of air traffic control sector capacity based on air traffic controller workload, *Transportation Planning and Technology* 20 (1997) 311–335.

[16] P. Di Mascio, R. Carrara, L. Frasacco, E. Luciano, A. Ponziani, L. Moretti, How the tower air traffic controller workload influences the capacity in a complex three-runway airport, *International journal of environmental research and public health* 18 (2021) 2807.

- [17] L. Adacher, M. Flamini, E. Romano, Rerouting algorithms solving the air traffic congestion, in: AIP Conference Proceedings, volume 1836, AIP Publishing LLC, 2017, p. 020053.
- [18] A. Mukherjee, M. Hansen, A dynamic rerouting model for air traffic flow management, *Transportation Research Part B: Methodological* 43 (2009) 159–171. doi:<https://doi.org/10.1016/j.trb.2008.05.011>.
- [19] S. Hamdan, A. Cheaitou, O. Jouini, T. A. Granberg, Z. Jemai, I. Alsyouf, M. Bettayeb, B. Josefsson, Central authority–controlled air traffic flow management: An optimization approach, *Transportation Science* 56 (2022) 299–321.
- [20] J.-R. Künnen, A. K. Strauss, N. Ivanov, R. Jovanović, F. Fichert, Leveraging demand–capacity balancing to reduce air traffic emissions and improve overall network performance, *Transportation Research Part A: Policy and Practice* 174 (2023) 103716.
- [21] O. Rodionova, H. Arneson, B. Sridhar, A. Evans, Efficient trajectory options allocation for the collaborative trajectory options program, in: 2017 IEEE/AIAA 36th Digital Avionics Systems Conference (DASC), IEEE, 2017, pp. 1–10.
- [22] O. Netto, J. Silva, M. Baltazar, The airport a-cdm operational implementation description and challenges, *Journal of Airline and Airport Management* 10 (2020) 14–30.
- [23] J. Im, J. Ahn, Decentralized free-flow traffic management based on nash equilibrium, *Journal of Aerospace Information Systems* 20 (2023) 195–203.
- [24] J. Im, Y. Yu, D. Fridovich-Keil, U. Topcu, Coordination in noncooperative multiplayer matrix games via reduced rank correlated equilibria, *IEEE Control Systems Letters* 8 (2024) 1637–1642.
- [25] J. Im, F. Fotiadis, D. Delahaye, U. Topcu, D. Fridovich-Keil, Noncooperative equilibrium selection via a trading-based auction, *arXiv preprint arXiv:2502.03616* (2025).
- [26] V. Vaze, C. Barnhart, Modeling airline frequency competition for airport congestion mitigation, *Transportation Science* 46 (2012) 512–535.
- [27] V. Vaze, R. Harder, A game-theoretic modeling approach to air traffic forecasting, in: 12th USA/Europe Air Traffic Management R and D Seminar, 2017.
- [28] M. Hansen, Airline competition in a hub-dominated environment: An application of noncooperative game theory, *Transportation Research Part B: Methodological* 24 (1990) 27–43.
- [29] K. Barker, S. Lakshminarahan, N. Ghorbani-Renani, A. Rangrazjeddi, A. D. González, R. Wood, J. Demagalski, Hf002: Applied game theory to enhance air traffic control training (????).
- [30] K. Tumer, A. Agogino, Improving air traffic management with a learning multiagent system, *IEEE Intelligent Systems* 24 (2009) 18–21.
- [31] M. Xiao, C. Hong, K. Cai, Optimizing the safety-efficiency trade-off on nationwide air traffic network flow using cooperative co-evolutionary paradigm, *Scientific Reports* 15 (2025) 20377.

- [32] A. Klein, P. Kopardekar, M. Rodgers, H. Kaing, " airspace playbook": Dynamic airspace reallocation coordinated with the national severe weather playbook, in: 7th AIAA ATIO Conf, 2nd CEIAT Int'l Conf on Innov and Integr in Aero Sciences, 17th LTA Systems Tech Conf; followed by 2nd TEOS Forum, 2007, p. 7764.
- [33] A. Klein, M. D. Rodgers, K. Leiden, Simplified dynamic density: a metric for dynamic airspace configuration and nextgen analysis, in: 2009 IEEE/AIAA 28th Digital Avionics Systems Conference, IEEE, 2009, pp. 2–D.
- [34] Y. Shoham, K. Leyton-Brown, Multiagent systems: Algorithmic, game-theoretic, and logical foundations, Cambridge University Press, 2008.
- [35] B. Swenson, R. Murray, S. Kar, On best-response dynamics in potential games, SIAM Journal on Control and Optimization 56 (2018) 2734–2767.
- [36] S. Arefizadeh, A. Nedich, G. Dasarathy, On characterizations of potential and ordinal potential games, arXiv preprint arXiv:2405.06253 (2024).
- [37] T. M. Inc., Global optimization toolbox version: 24.2 (r2024b), 2024.
- [38] H. Yang, D. Delahaye, C. Ma, S. Alam, Large-scale congestion mitigation in european airspace, in: Proceedings of the SESAR Innovation Days 2025, Lake Bled, Slovenia, 2025. Under review.